1

Scale-Up of a Cold Flow Model of FICFB Biomass Gasification Process to an Industrial Pilot Plant – Example of Dynamic Similarity

Jernej Mele
Faculty of mechanical engineering/Bosio d.o.o.
Slovenia

1. Introduction

In this chapter we are introducing the research of particles hydrodynamics in a cold flow model of **F**ast **I**nternal **C**irculating **F**luidized **B**ed (FICFB) biomass gasification process and its scale-up to industrial pilot plant. A laboratory unit has been made for the purposes of experimental research. The laboratory unit is three times smaller than the later pilot plant. For a reliable observation of the flow process, similar flow conditions must be created in the laboratory unit and the pilot plant. The results of the laboratory model will be similar to those of the actual device if geometry, flow and Reynolds numbers are the same. Therefore, there is no need to bring a full-scale gasificator into the laboratory and actually test it. This is an example of "dynamic similarity".

FICFB biomass gasification is a process for producing high caloric synthesis gas (syngas) from solid Hydrocarbons. The basic idea is to separate syngas from flue gas, and due to the separation we have a gasification zone for endothermic reactions and a riser for exothermic reactions. The bed material circulates between these two zones and serves as a heat carrier and a catalyst.

While researching the 250kW fluidized bed gasification pilot plant certain questions concerning particle dynamics in gas flows control arose. There is a zone where fluidized bed conditions are made with superheated steam, pneumatic transport with hot air and a pair of secondary gas inlets of CO_2. These particle flows are difficult to describe with mathematical models. This is the main reason why the three-times smaller cold-flow laboratory unit has been made. The hydrodynamics of particles will be studied in the air flow at arbitrary conditions. Flow conditions in the laboratory unit and pilot plant must be similar for a reliable evaluation of the process in the pilot plant.

2. Laboratory unit

The laboratory unit is a device three times smaller than the pilot plant. Its main purpose is to simulate the hydrodynamic process of FICFB gasification in a cold flow. It is made from stainless steel and in the case of the parts that are of greatest interest to the present study is made of glass, so that the particle behaviour may be observed. Fig. 1 shows a model of laboratory unit. Its main elements are:

- Reactor (A),
- Riser (B),
- Cyclone (C),
- Siphon (D),
- Chute (E),
- Gas distributor (J_1 and J_2),
- Auxiliary inlets (I_1 and I_2).

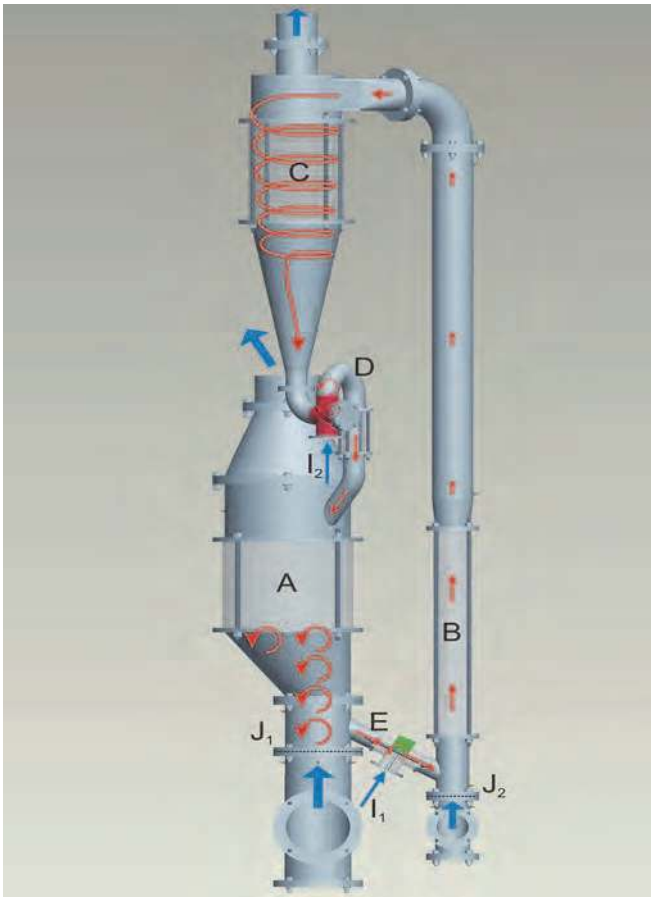

Fig. 1. 3D model of laboratory unit

Firstly, let us look at the process. There are two gas distributors at the bottom of the reactor and riser, through which air is blown vertically. The pneumatic transport of the particles takes place in the riser, where they are separated from the air flow in cyclone and finally gathered in siphon. The second auxiliary inlet acts to fluidize the gathered particles and transport them to the reactor. Here, the fluidized bed is created with the upward blowing air. From here, the particles are transported to the riser through the chute and the speed of transportation is regulated by means of the first auxiliary inlet.

	Laboratory unit	Pilot plant
$D_{gas,1}$ [mm]	100	300
$D_{gas,2}$ [mm]	190	600
D_{comb} [mm]	50	150
H_{comb} [mm]	1500	4500

Table 1. Main dimensions of laboratory unit and pilot plant

We are primarily interested in how to establish a stationary and self-sustainable process. In the laboratory unit there are glass parts through which the process in course can be directly observed. However, in the hot flow model we will not be able to see what happens inside the pilot plant, and therefore our control system must be able to initiate the process, keep it in a stationary state and halt it on the basis of measured data such as relative pressure and flow velocities. For this mater, our laboratory unit consists of 7 pressure and 2 flow velocity measuring points. Fig. 2 details the positions of the pressure places.

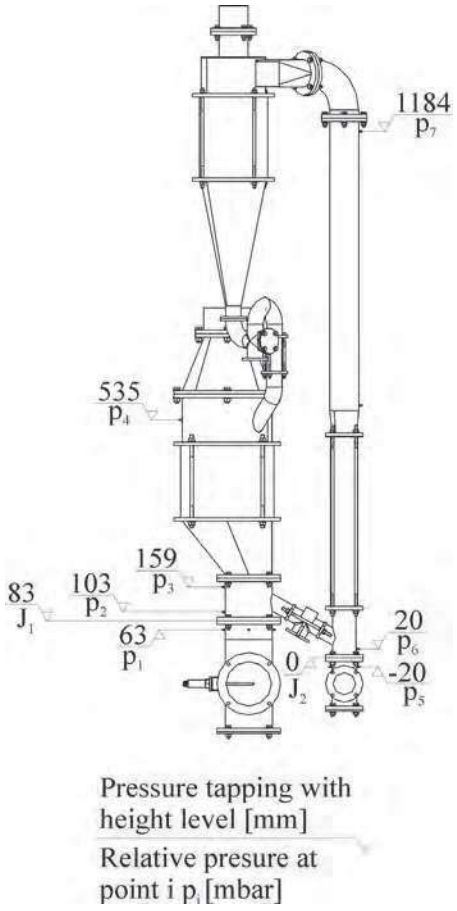

Fig. 2. Openings for the measuring of relative pressure

Trough experiments on the laboratory unit the effectiveness of elements will be studied so as to enable the correction and improvement of any construction flaws they contain. Fig. 3 shows the laboratory unit that will be used for studying the flow process. There are 7 places for pressure, 2 for temperature and 2 for gas flow measurements. For the proper operation of our solid flow system it is vital that the particles are maintained in dynamic suspension as settling down the particles can clog both the measuring openings and injection nozzles. Thus it is essential to design such systems with special care. All measurements involving the risk of clogging the measuring opening must be taken outside the solid flow zone if possible – gas flow velocity measurements with the Pitot tube must be taken in the gas pipeline before gas enters thru distributor. It is highly desirable for all measuring openings to be small and positioned rectangular to the direction of flow (Nicastro & Glicksman, 1982).

Fig. 3. Laboratory unit

2.1 Distributor

For the distributor 3 metal nets with openings of 225 μm have been used, with ceramic wool of 8mm placed in between as shown in fig. 4. We tried to achieve a sufficient pressure drop as to attain equal flow through the openings. According to Agarwal recommendation (Kunii & Levenspiel, 1991; Nicastro & Glicksman, 1982), the pressure drop across distributors must

be 10 % of the pressure drop across the bed, with a minimum of 35 mm H_2O. With this we are in approximate agreement. At higher pressure drops across the distributor we get more particulate or smooth fluidization with less channelling, slugging and fluctuation in density. The pressure drop across the distributor is shown in fig. 5.

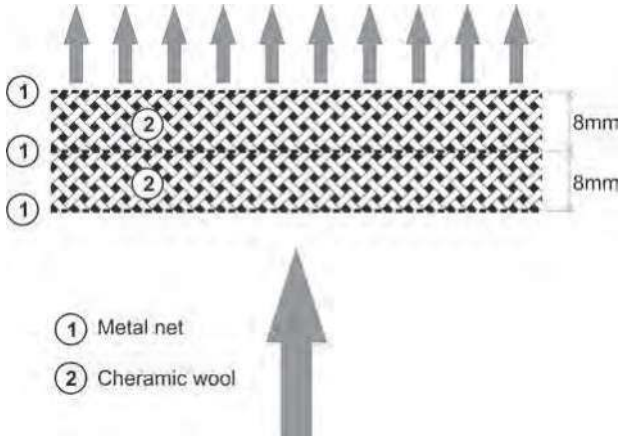

Fig. 4. Distributor structure

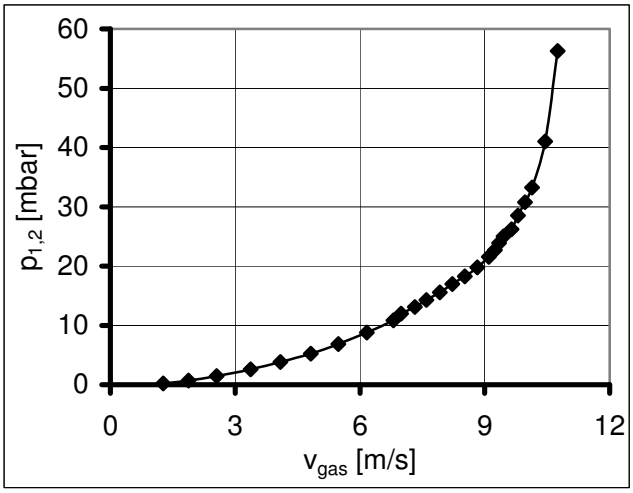

Fig. 5. Pressure drop across the distributor with blowing of air

2.2 Cyclone

In our case, the cyclone separator is placed behind the riser to separate the particles from the air flow. It has to be able to separate particles larger than 50 µm. For these conditions these particles are considered large as cyclones are often used for the removal of particles of about 10 µm diameter or larger from air streams. Our model is shown in fig. 6.

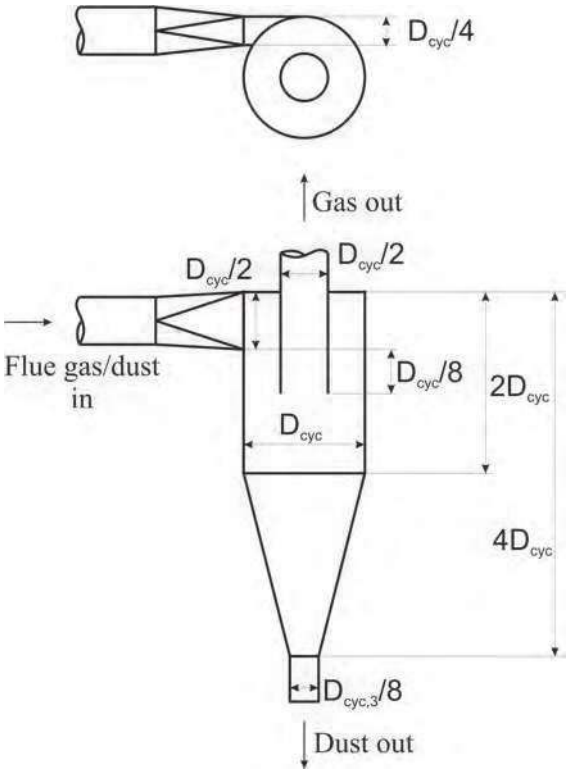

Fig. 6. The characteristic dimensions of cyclone

We dimensioned our cyclone according to Perry (Perry, 1988). $D_{p,50}$ is the particle size at which 50 % of solids of a given size are collected by the cyclone.

$$D_{p,50} = \sqrt{\frac{9 \cdot \eta_g \cdot B_{cyc}}{\pi \cdot N_s \cdot v_g \cdot \left(\rho_p - \rho_g\right)}} \tag{1}$$

By rearranging the equation (1), we obtain the following expression:

$$B_{cyc} = \frac{{D_{p,50}}^2 \cdot \pi \cdot N_s \cdot v_g \cdot \left(\rho_p - \rho_g\right)}{9 \cdot \eta_g} \tag{2}$$

The width of the cyclone entering the opening and the characteristic diameter are correlated by the following expression:

$$B_{cyc} = \frac{D_{cyc}}{4} \tag{3}$$

The diameter of our cyclone is 150 mm. Smaller particles, which are not separated in cyclone are being collected in a filter placed on the cyclone gas exit.

3. Basic equations for describing the fluidized state and similarity of flows

3.1 Reynolds number

The goal herein is to compare flows in the laboratory unit to those in the pilot plant. In order for the two flows to be similar they must have the same geometry and equal Reynolds numbers. When comparing fluid behaviour at homologous points in a model and a full-scale flow, the following holds:

Re(laboratory unit) = Re(Scale-up pilot plant)

The Reynolds number of particles can be determined by the following equation (Kunii & Levenspiel, 1991):

$$\mathrm{Re}_p = \frac{D_p \cdot v_g \cdot \rho_g}{\eta_g} \tag{4}$$

For achieving the required similarity, the following conditions must be also fulfilled:

$$\frac{p}{\rho_g \cdot {v_g}^2} = \frac{p_{g,ar}}{\rho_{g,ar} \cdot {v_{g,ar}}^2} \tag{5}$$

3.2 Minimal fluidizing velocity

The fluidization state starts when the drag force of by upward moving gas equals the weight of the particles (Oman, 2005)

$$F_{g\_p} = \frac{1}{2} \cdot C_x \cdot A_p \cdot \rho_p \cdot {v_g}^2 \tag{6}$$

or

$$\Delta p \cdot A_t = \left(A_t \cdot L_{mf}\right)\left(1-\varepsilon_{mf}\right)\left[\left(\rho_s - \rho_g\right)\frac{g}{g_c}\right] \tag{7}$$

By rearranging equation (7), for minimum fluidizing conditions we find the following expression (Kunii & Levenspiel, 1991),

$$\frac{\Delta p_{mf}}{L_{mf}} = \left(1-\varepsilon_{mf}\right)\left(\rho_s - \rho_g\right)\frac{g}{g_c} \tag{8}$$

Voidage in fluidized bed ε_{mf} is larger than in the packed bed and it can be estimated experimentally from a random ladling sample. For small particles and low Reynolds numbers the viscous energy losses predominate and the equation simplifies to (Kunii & Levenspiel, 1991):

$$v_{mf} = \frac{\left(\Phi_s \cdot D_p\right)^2}{150} \cdot \frac{\rho_p - \rho_g}{\eta_g} \cdot g \cdot \frac{{\varepsilon_{mf}}^2}{\left(1-\varepsilon_{mf}\right)} \tag{9}$$

for $\mathrm{Re}_p < 20$

For large particles only the kinetic energy losses need to be considered:

$$v_{mf} = \sqrt{\frac{\Phi_s \cdot D_p}{1{,}75} \cdot \frac{(\rho_p - \rho_g)}{\eta_g} \cdot g \cdot \varepsilon_{mf}{}^3} \tag{10}$$

for $Re_p > 1000$.
If Φ_S and ε_{mf} are unknown, the following modifications suggested by Wen and Yu (Kunii & Levenspiel, 1991) are used:

$$\frac{1 - \varepsilon_{mf}}{\Phi_S{}^2 \cdot \varepsilon_{mf}{}^2} \cong 11 \tag{11}$$

$$\frac{1}{\Phi_S \cdot \varepsilon_{mf}{}^3} \cong 14 \tag{12}$$

Equations (9) and (10) can now be simplified to:

$$v_{mf} = \frac{D_p{}^2 \cdot \left(\rho_p - \rho_g\right) \cdot g}{1650 \cdot \eta_g} \tag{13}$$

for $Re_p < 20$

$$v_{mf} = \sqrt{\frac{D_p \cdot g \cdot (\rho_p - \rho_g)}{24{,}5 \cdot \rho_g}} \tag{14}$$

for $Re_p > 1000$.

3.3 Terminal velocity

The upper limit of gas flow rate is approximated by the terminal (free fall) velocity of the particles, which can be estimated from the fluid mechanics (Kunii & Levenspiel, 1991):

$$v_t = \sqrt{\frac{4 \cdot g \cdot D_p \cdot (\rho_p - \rho_g)}{3 \cdot \rho_g \cdot C_x}} \tag{15}$$

There are spherical and non-spherical particle shapes in the bed and each of them has a different C_x value. If we combine equations (4) and (15) we get the velocity independent group:

$$C_x \, \mathrm{Re}_p{}^2 = \frac{4 \cdot g \cdot D_p{}^3 \cdot \rho_g \cdot \left(\rho_p - \rho_g\right)}{3 \cdot \eta_g{}^2} \tag{16}$$

An alternative way of finding v_t for spherical particles uses analytical expressions for the drag coefficient C_x (Kunii & Levenspiel, 1991).

$$C_x = \frac{24}{\mathrm{Re}_p} \quad \text{for} \quad Re_p < 0{,}4 \tag{17}$$

$$C_x = \frac{10}{\sqrt{\mathrm{Re}_p}} \quad \text{for} \quad 0{,}4 < \mathrm{Re_p} < 500 \tag{18}$$

$$C_x = 0{,}43 \quad \text{for} \quad 500 < \mathrm{Re_p} < 200000 \tag{19}$$

But still no simple expression can represent the experimental findings for the entire range of Reynolds numbers, so by replacing these values C_x in equation (16) we obtain:

$$v_t = \frac{\left(\rho_p - \rho_g\right) \cdot g \cdot {D_p}^2}{18 \cdot \eta_g} \tag{20}$$

for $\mathrm{Re_p} < 0{,}4$

$$v_t = \sqrt[3]{\frac{4}{225} \cdot \frac{\left(\rho_p - \rho_g\right)^2 \cdot g^2}{\eta_g \cdot \rho_g}} \cdot D_p \tag{21}$$

for $0{,}4 < \mathrm{Re_p} < 500$
and

$$v_t = \sqrt{\frac{3{,}1 \cdot D_p \cdot g \cdot (\rho_p - \rho_g)}{\rho_g}} \tag{22}$$

for $500 < \mathrm{Re_p} < 200000$.

3.4 Determining density

In the pilot plant we will have multiple gas mixtures at different temperatures due to chemical reactions. For our calculations the density for these mixtures will be determined by the following equation (Oman et al., 2006):

$$\rho_g = \left(\sum_i \frac{w_i}{\rho_i} \right)^{-1} \tag{23}$$

To calculate the density of the gas mixture at an arbitrary temperature and an arbitrary pressure the density under normal condition must be calculated according to equation (24), with the obtained value being converted to density at the required parameters:

$$\rho_{g,ar} = \rho_g \cdot \frac{p_{g,ar}}{p_n} \cdot \frac{T_n}{T_{g,ar}} \tag{24}$$

3.5 Pressure drops

With increased gas velocity of the small solid particles across the bed a characteristic state occurs. Pressure drop starts to increase, reaching its maximum value Δp_{mf} at minimum fluidization velocity v_{mf}. At this point only part of the bed is fluidized. When the bed is fully fluidized (at v_{mff}), the pressure drop is reduced to Δp_{mff} and is almost constant until gas reaches terminal velocity. If the velocity is still increasing, the particles start transporting

pneumatically and pressure drop reduces rapidly to 0. By rearranging equation (8), we obtain the following expression (Kunii & Levenspiel, 1991):

$$\Delta p_{mf} = \left(1 - \varepsilon_{mf}\right)\left(\rho_s - \rho_g\right) \cdot g \cdot L_{mf} \tag{25}$$

The expression can also be extended to the fully fluidized state (Kaewklum & Kuprianov, 2008):

$$\Delta p_{mff} = \left(1 - \varepsilon_{mff}\right)\left(\rho_s - \rho_g\right) \cdot g \cdot L_{mff} \tag{26}$$

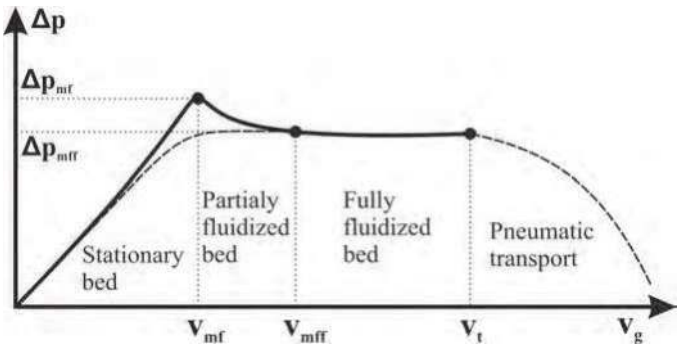

Fig. 7. The change in pressure drop relative to gas velocity for Not-too-Small Uniformly Sized Particles (Kunii & Levenspiel, 1991)

A somewhat different differential pressure characteristic occurs with a wide size distribution of particles, which are usually present in industrial processes. When the gas velocity increases through the bed of solids, the smaller particles start to fluidize and slip into the void spaces between the larger particles, while the larger particles remain stationary (Kunii & Levenspiel, 1991) (see Fig. 8). However, after a full fluidization of bed material ($v_g > v_{mff}$), with increasing air velocity, pressure drop mainly remains constant.

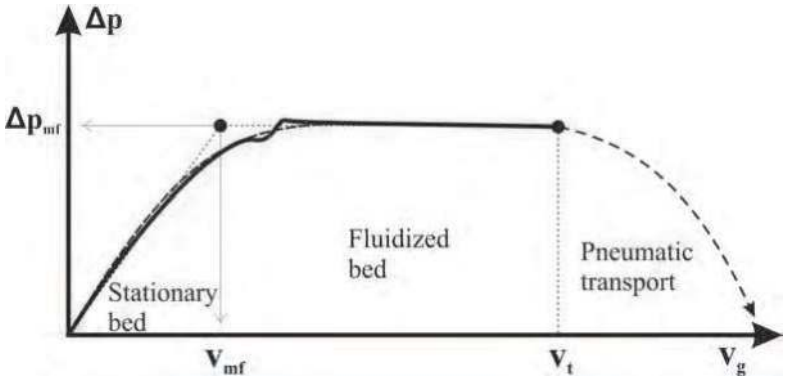

Fig. 8. The change in pressure drop relative to gas velocity for Wide Size Distribution of Particles (Kunii & Levenspiel, 1991)

3.6 Mass flows and conservation of mass

For a regular flow process we have to ensure proper gas flows at the inlets. Through defining minimal fluidizing and terminal velocities, we can estimate the mass flow of the air reactor and riser by applying the following relations:

$$\varphi_{m\_g} = \rho_g \cdot v_g \cdot \frac{\pi \cdot D_{tube}{}^2}{4} \tag{27}$$

$$\varphi_{V\_g} = \frac{\varphi_{m\_g}}{\rho_g} \tag{28}$$

It is extremely important to ensure that there are no mass losses between the ventilator and the reactor. It can be assumed:

$$v_g \cdot \frac{D_{gas,2}{}^2 \cdot \pi}{4} = v_{g,ref} \cdot \frac{D_{tube}{}^2 \cdot \pi}{4} \tag{29}$$

4. Calculation analyses

On the basis of the previously-mentioned equations, we can make an estimation of flow conditions in the reactor and riser. We have made a tabular comparison of physical properties between the laboratory unit and pilot plant in tables 2 and 3. The comparison is based on the established equality of Reynolds numbers. As mentioned in chapter 3.1. "In order for two flows to be similar they must have the same geometry and equal Reynolds numbers". In the laboratory unit, flows will be made with upward-blowing air at room temperature whereas in the pilot plant the fluid bed will be made with inlet of superheated steam and pneumatic transport with hot air blowing at 550 °C.

	Reactor	
	Laboratory unit	Pilot plant
Gas	Air	Steam / Syngas
T [°C]	30	550 / 800
D_p [µm]	200	600
ρ_p [kg/m³]	8250	3025
ρ_g [kg/m³]	1,204	0,288 / 0,192
η_g [Pas]	1,8·10-5	3,1·10-5 / 4,6·10-5
$v_{Re<20}$ [m/s]	0,11	0,21 / 0,14
$v_{Re>1000}$ [m/s]	0,75	1,58 / 1,95
Φ_m [kg/h]	6,4	158,9
Φ_V [m³/h]	5,4	548,5
Re_p	9,8	9,0 /4,9

Table 2. Physical properties of gas in Reactor

In the meantime endothermic chemical reactions of pyrolisys, a water-gas-shift reaction will take place in the reactor while exothermic combustion occurs in the riser. Flue gases will

have a the temperature of around 1000 °C on exiting the combustor and syngas a temperature of approximately 800 °C at the reactor's point of exit. Gases in the pilot plant will have lower densities and higher viscosities than the air in the laboratory unit. The bed material will be Olivine with D_p = 600 µm. In order to establish similar conditions, we have to use smaller and denser particles. We have chosen brass particles with D_p = 200 µm . Simulation will also be tested with quartz sand and olivine.

	Riser	
	Laboratory unit	Pilot plant
Gas	Air	Air / Flue gas
T_g [°C]	30	550 / 1000
D_p [µm]	200	600
ρ_p [kg/m^3]	8250	3025
ρ_g [kg/m^3]	1,204	0,61/0,294
η_g [Pas]	1,8·10-5	3,8·10-5/4,7·10-5
v_{Re}<0.4 [m/s]	10,1	15,7/12,6
$v_{0.4<Re<500}$ [m/s]	3,6	5,3/6,2
$v_{500<Re<200000}$ [m/s]	6,6	9,6/13,7
Φ_m [kg/h]	47,7	154,2
Φ_V [m^3/h]	39,6	524,5
Re_p	46,6	50,8 / 23,3

Table 3. Physical properties of gas in Riser

On the basis of studied flow velocities, mass flows, as well as pressure drops through air distributors and fluid beds at different points of the laboratory unit, we may anticipate the similar results in the pilot plant.

5. Experimental work

Firstly, we have to establish the fluidized bed in the reactor. The particles will fill the chute and the lower part of the riser. The chute is installed at the bottom of the reactor and riser and has an inclination angle. The fluidizing of the particles in the chute will then be started, along with the simultaneous initialization of the pneumatic transport of the particles. When sufficient material has been gathered in the siphon, the particles must be transported back to the reactor with the help of the first auxiliary inlet. The particles are now at their starting point. We must achieve a pressure at the bottom of the fluidized bed p_2 which is larger than that at the point where the chute connects to the riser p_6. The gas flow direction will be from the reactor to the riser, pushing the particles in the desired direction. At the top of the fluidized bed we have pressure p_4 which has to be lower than p_7, so the particles can now travel back to the reactor. But there has to be enough material in the siphon at all times in order to prevent the mixing of gases between the zones. Therefore, the siphon has to serve as seal gap for gases but not for material. The more gas goes through the siphon the lower the caloric value of the gas will be. Experiments will show how pressures are distributed across the system. Fig. 9 shows which measured pressures are of greatest interest for our purposes.

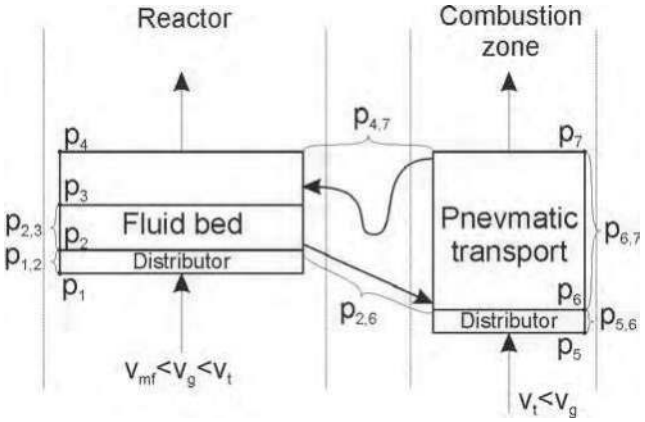

Fig. 9. Measuring scheme

By way of example, we will look at the experiment with quartz sand. The size of the particles used for simulation is shown in fig. 13. The particles have an average diameter of about 200 μm. A series of measurements were made and pressure drops at different bed heights taken. Fig. 10 represents a comparison of pressure drop across the bed in the reactor with the gas velocity for different bed heights.

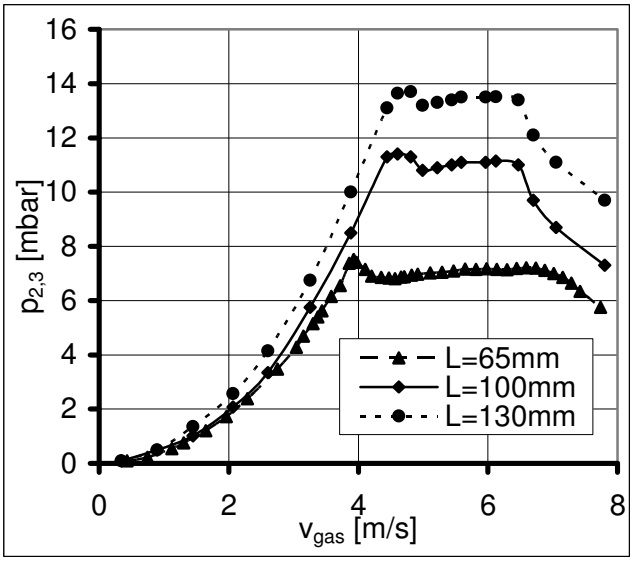

Fig. 10. Pressure drops over fluidized bed

In lower beds less aggregative bubbling occurs and results closer to calculated values are obtained. Nevertheless, still there is a lot of deviation between them. In addition, there is some leakage of gas from the reactor through chute to the riser and as the Pitot tubes are placed in front of gas entering each zone those velocities do not represent the real situation,

although the mass flow of air blown through unit is quite as predicted. However, gas velocity is almost impossible to measure within the laboratory unit because attempts to do so would inevitably lead to bed material clogging the measure openings in the device. Having said that, our assessment and purpose is to define and achieve a stationary process on the basis of the measuring system. The measured quantities are presented in table 4.

Symbol	Value	[unit]
p_1	34.4	mbar
p_2	11.3	mbar
p_3	0.2	mbar
p_4	0.1	mbar
p_5	6.2	mbar
p_6	3.9	mbar
p_7	3.2	mbar
v_{gas}	5.1	m/s
v_{comb}	9	m/s

Table 4. Measurements results

Comparisons of error between calculations and experimental results of pressure drops are presented in fig. 11 and 12. Through the application of the mathematical models we find that pressure drops can be predicted within a 20 % error margin. For example let us compare results between calculated and experimental values of pressure drop across 100 mm bed of quartz sand at minimum fluidization conditions. Calculating pressure drop according to equation 23 gives us 12.5 mbar, where physical properties are as follows: ρ_p = 2650 kg/m^3, ρ_g = 1.204 kg/m^3, ε_{mf} = 0.55, L_{mf} = 110 mm ang g = 9,81 m/s^2. Bed height increases for 10 mm and so does consecutive voidage. A series of measurements gives us the average value for pressure drop which is $p_{2,3}$ = 11.4 mbar. As follows from this, the error of our prediction was 8.8 %.

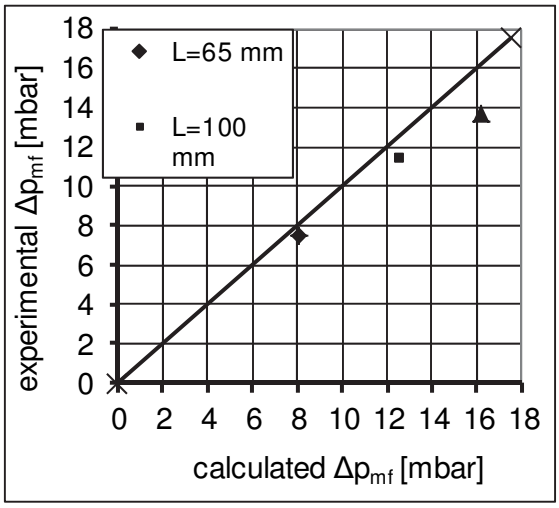

Fig. 11. The comparison of experimental and calculated Δp_{mf} for 200 μm quartz sand

For calculating pressure drops across fully fluidized bed we use equation 26. The only difference comes with a little higher bed and voidage, which remain almost constant with increasing gas velocity to terminal velocity. So if we consider that L_{mff} = 115 mm and ε_{mff} = 0.62 than pressure drop equals 11.4 mbar. With the comparison to the experimental value, which is 10.8 mbar, a 5.2 % error of prediction occurs. Error highly increases in aggregative and slugging mode of fluidization.

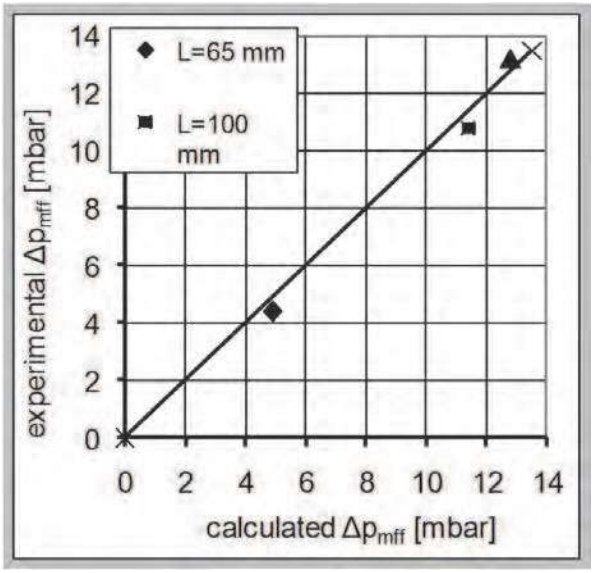

Fig. 12. Comparison of experimental and calculated Δp_{mff} for 200 µm quartz sand

Relative pressures were measured at a stationary state. One of the experiments was made when testing the process with quartz sand where the average particle diameter was about 200 µm. The stationary bed height in the reactor was 100 mm and the mass of sand used at simulation was 4.25 kg. When minimum fluidization conditions were obtained, the bed height increased by approximately 15 mm. A series of repeated measuring were carried out

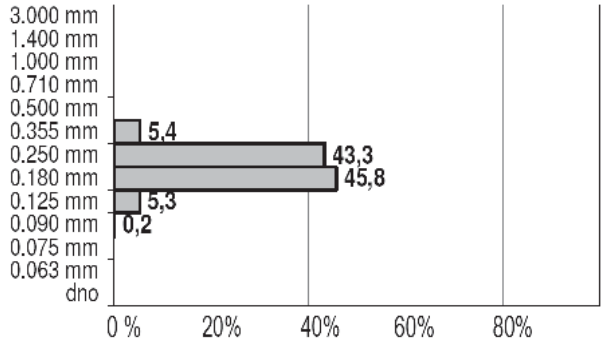

Fig. 13. The size of the particles used for simulation

and the average relative pressure at the bottom of the fluid bed was p_2 = 11.3 mbar, with p_3 = 0.2 mbar the average value at the top. As follows from this, the pressure drop across fluidized bed was $p_{2,3}$ = 11.1 mbar. Air flow had an average temperature of 25 °C. Inlet gas velocity was about 5.1 m/s in the reactor and 9 m/s in the riser. We found a higher gas velocity for fluidization than calculated, due to a certain amount of air passing through the chute to the riser. This also provides the explanation as to why the measured terminal velocity in the riser was a little lower than anticipated, as the loss of air from the reactor helped increase the air speed in the riser – resulting in the aforementioned lower value.

6. Comparison to the previously used methods

Modern gasification is occurring in fluidized beds. Its advantage is using most fuels (wood, peat and coal) including agriculture "waste" such as straw, corn stover and manure. It has a potential to use municipal waste, such as garbage, it is quicker in response and it has shorter start up time. It lends itself to complete combustion applications which would allow it to use liquid wastes, such as used engine oil, non-recyclable plastics, junk mail & old shoes and garbage for the generation of heat. However, there is a problem of complex design. Still, nowadays most research efforts are being made on fluidization bed technology.
We tested a system very similar to the one tested by G. Löffler, S. Kaiser, K. Bosch, H. Hofbauer (Kaiser S. et al., 2003) with a minor difference. Our reactor had an eccentric diffuser which proved not to be a successful idea (Mele, J. et al., 2010). That is why in future research we are planning to test a reactor with a conical bed similar to those used by Kaewklum and Kuprianov. Our mathematical model is based on the derivation of Ergun's equation (Kunii & Levenspiel, 1991). L. Glicksman pointed out that for designing an accurate scale model of a given bed all of the independent non-dimensional parameters must be identical, such as considering the case where fluidized bed is operated at an elevated temperature of flue gas or at arbitrary conditions with air (Glicksman, 1982). Our work is also based on attaining similar non-dimensional parameters such as Reynolds and Euler numbers. The Freude number based on the minimum velocity, (v_{mf}/dp_g) has been proposed as the parameter to characterize the boundary between particulate and aggregative fluidization and the Archimedes number has been used to correlate a wide array of phenomena (Zabrodsky, 1966).

7. Conclusions

By observing the CFB processes in a three-times smaller laboratory unit with air flow the size and density of particles has been determined. The preferred option was to use brass powder with an average particle diameter of 200 μm. The assumption of particle flow similarity is based on a direct comparison of Reynolds numbers. In this case the Re_p are 9.8 and 9.0 in reactor and 46.6 and 50.8 in the riser. There is a 10 % difference between Re_p in both cases. Chemical reactions cause variations in temperature, density, and dynamic viscosity all of which affect Re_p. If we compare Re_p 9.8 and 4.9 at the reactor exit 46.6 and 23.3 at the top of the riser exit, we can see that Re_p changes by 50 % and the similarity at this point is actually questioned. By way of example, the experiment carried out with quartz sand was presented. When the process is stabilized and a smooth circulation is established, then pressure drops are as follows: $p_{2,3}$ = 11.2 mbar, $p_{6,7}$ = 0.7 mbar, $p_{2,6}$ = 7.4 mbar and $p_{4,7}$ = -3.1 mbar. This result set can be characterized as $p_2 > p_6$ and $p_4 < p_7$. Pressures are as expected and gas flows are in the appropriate directions. Through the application of the mathematical

models we have, pressure drops can be predicted to within a 20% error margin. The experiments highlighted one major problem, namely that the cylindrical tube and asymmetric enlargement of the tube didn't prove to be a successful construction for the reactor. With beds higher than 13 cm fluidized beds are in aggregative or bubbling fluidization states. In turn, at bed heights over 30 cm even a slugging state is attained. The solution at this point is a conical bed design in accordance with Kaewklum and Kuprianov, 2008.

8. Symbols

A_p	Cross-section of particle	[m²]
A_t	Tube cross-section	[m²]
B_{cyc}	Width of rectangular cyclone inlet dutch	[m]
C_x	Drag coefficient	
D_{cyc}	Characteristic cyclone diameter	[m]
D_{comb}	Riser diameter	[mm]
$D_{gas,1}$	Diameter of reactor upper segment	[mm]
$D_{gas,2}$	Diameter of reactor lower segment	[mm]
D_p	Diameter of particle	[µm]
$D_{p,50}$	Particle diameter at which 50% of particles are collected by cyclone	[µm]
D_{tube}	Inside tube diameter	[mm]
F_{g_p}	Gravity of particle	[N]
g	Gravity acceleration [9,81 m/s²]	
g_c	Conversion factor [9,81gm m/s² wt]	
H_{comb}	Riser height	[mm]
i	Natural number	
j	Natural number	
L	Stationary bed height	[m]
L_{mf}	Bed height at minimum fluidization condition	[m]
L_{mff}	Bed height at minimum fully fluidized state	[m]
N_s	Number of turns made by gas stream in a cyclone separator	
p	Pressure	[Pa]
$p_{g,ar}$	Pressure at arbitrary conditions	[Pa]
p_i	Relative pressure in point i	[Pa]
$p_{i,j}$	Differential pressure between points i and j	[Pa]
p_j	Relative pressure in point j	[Pa]
p_n	Pressure at normal conditions	[Pa]
Re_p	Particle Reynolds number	
$T_{g,ar}$	Temperature at arbitrary conditions	[°C]
T_n	Temperature at normal conditions	[°C]
v_{comb}	Gas velocity in riser	[m/s]
v_g	Gas velocity	[m/s]
$v_{g,ref}$	Gas velocity measured with pitot tube or orifice in tube before gas entering reactor	[m/s]
v_{gas}	Gas velocity in gasification zone	[m/s]

v_{mf}	Minimal fluidization velocity	[m/s]
v_{mff}	Minimal velocity of full fluidization	[m/s]
v_t	Terminal velocity	[m/s]
Δp	differential pressure	[Pa]
Δp_{mf}	differential pressure at minimum fluidization	[Pa]
Δp_{mff}	differential pressure at full fluidization	[Pa]
ε	Bed voidage	
ε_{mf}	Bed voidage at minimum fluidization	
ε_{mff}	Bed voidage at full fluidization	
η_g	Dynamical viscosity of gas	[Pa·s]
$\eta_{g,ar}$	Dynamical viscosity of gas at arbitrary conditions	[Pa·s]
η_n	Dynamical viscosity of gas at normal conditions	[Pa·s]
ρ_g	Density of gas	[kg/m^3]
ρ_p	Density of particle	[kg/m^3]
Φ_m	Mass flow	[kg/h]
Φ_{m_g}	Mass flow of gas	[kg/h]
Φ_V	Volume flow	[m^3/h]
Φ_{V_g}	Volume flow of gas	[m^3/h]

9. References

Glicksman, L. R. (1982). Scaling Relationships For Fluidized Beds, Chemical engineering science, 39, 1373-1384

Kaewklum, R. & Kuprianov, V. I. (2008). *Theoretical And Experimental Study On Hydrodynamic Characteristic Of Fluidization In Air-Sand Conical Beds*, Chemical Engineering Science 63 1471-1479

Kaiser, S.; Löffler, G.; Bosch, K.; Hofbauer, H. (2003). *Hydrodynamics of a Dual Fluidized Bed Gasifier - Part Ii: Simulation of Solid Circulation Rate, Pressure Loop and Stability*, Chemical Engineering Science, 58, 4215 – 4223

Kunii, D. & Levenspiel, O.; (1991). *Fluidization Engineering - Second edition*, John Wiley & Sons, inc.,

Löffler G., Kaiser S., Bosch K., Hofbauer H. (2003). *Hydrodynamics of a Dual Fluidized - Bed Gasifier - Part I : Simulation of a Riser With Gas Injection and Diffuser*, Chemical Engineering Science, 58, 4197 – 4213

Mele, J.; Oman, J.; Krope, J. (Jan. 2010). *Scale-up of a cold flow model of FICFB biomass gasification process to an industrial pilot plant - hydrodynamics of particles,* WSEAS transactions on fluid mechanics, vol. 5, iss. 1, str. 15-24.

Nicastro, M. T. & Glicksman, L. R. (1982). *Experimental Verification of Scaling Relationships for Fluidized Beds*, Chemical engineering science, 39, 1373-1384

Oman J. (2005), *Generatorji Toplote*, University in Ljubljana, Faculty of mechanical engineering, Ljubljana,

Oman, J.; Senegačnik, A.; Mirandola, A. (2006). *Air, Fuels and Flue Gases: Physical Properties and Combustion Constants*, Edizioni Librerita Progeto, Padova, Italy

Perry, R. H. (1988). *Perry's Chemical Engineers Handbook (6th ed.)*, New York: McGraw Hill International Ed.

Zabrodsky, S. S. (1966). *Hydrodynamics And Heat Transfer In Fluidized Beds*, The MIT press, Cambrige

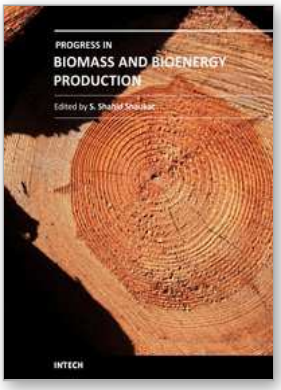

Progress in Biomass and Bioenergy Production

Edited by Dr. Shahid Shaukat

ISBN 978-953-307-491-7
Hard cover, 444 pages
Publisher InTech
Published online 27, July, 2011
Published in print edition July, 2011

Alternative energy sources have become a hot topic in recent years. The supply of fossil fuel, which provides about 95 percent of total energy demand today, will eventually run out in a few decades. By contrast, biomass and biofuel have the potential to become one of the major global primary energy source along with other alternate energy sources in the years to come. A wide variety of biomass conversion options with different performance characteristics exists. The goal of this book is to provide the readers with current state of art about biomass and bioenergy production and some other environmental technologies such as Wastewater treatment, Biosorption and Bio-economics. Organized around providing recent methodology, current state of modelling and techniques of parameter estimation in gasification process are presented at length. As such, this volume can be used by undergraduate and graduate students as a reference book and by the researchers and environmental engineers for reviewing the current state of knowledge on biomass and bioenergy production, biosorption and wastewater treatment.

How to reference

In order to correctly reference this scholarly work, feel free to copy and paste the following:

Jernej Mele (2011). Scale-up of a Cold Flow Model of FICFB Biomass Gasification Process to an Industrial Pilot Plant – Example of Dynamic Similarity, Progress in Biomass and Bioenergy Production, Dr. Shahid Shaukat (Ed.), ISBN: 978-953-307-491-7, InTech, Available from: http://www.intechopen.com/books/progress-in-biomass-and-bioenergy-production/scale-up-of-a-cold-flow-model-of-ficfb-biomass-gasification-process-to-an-industrial-pilot-plant-exa

INTECH
open science | open minds

InTech Europe
University Campus STeP Ri
Slavka Krautzeka 83/A
51000 Rijeka, Croatia
Phone: +385 (51) 770 447
Fax: +385 (51) 686 166
www.intechopen.com

InTech China
Unit 405, Office Block, Hotel Equatorial Shanghai
No.65, Yan An Road (West), Shanghai, 200040, China
中国上海市延安西路65号上海国际贵都大饭店办公楼405单元
Phone: +86-21-62489820
Fax: +86-21-62489821

© 2011 The Author(s). Licensee IntechOpen. This chapter is distributed under the terms of the Creative Commons Attribution-NonCommercial-ShareAlike-3.0 License, which permits use, distribution and reproduction for non-commercial purposes, provided the original is properly cited and derivative works building on this content are distributed under the same license.